Experiments
Учебен експеримент в природните науки

THERMODYNAMIC AND INTERFACIAL STUDIES ON CO-CRYSTALS OF NICOTINAMIDE - THIOUREA DRUG SYSTEM

Vishnu Kant, H. Shekhar
Veer Kunwar Singh University, India

Abstract. The present communication aims at investigating the Nicotinamide (NA) – Thiourea (TU) binary system in the solid state emphasizing thermodynamic and interfacial studies. It was found from the solid-liquid phase diagram of the system that an A 1:5 additive co-crystal formed at 161°C and two side by side eutectic solid dispersions E2 (mole fraction 0.407 of TU) and E1 (mole fraction 0.968 of TU) at 142°C and 116°C respectively. The activity coefficient model based on enthalpy of fusion was employed to calculate the excess thermodynamic properties that of g^E, h^E and s^E, which predict the nature of molecular interaction, ordering and stability between the components. The negative value of integral Gibbs free energy of mixing, ΔG^M for all the eutectic and non-eutectic solid dispersions favours the spontaneous mixing in all solid dispersions. The driving force of nucleation during solidification (ΔG_v) and the critical free energy of nucleation (ΔG^*) at different undercoolings have also been highlighted. The value of radius of critical nucleus (r^*) of solid dispersions has been found in *nm* scale which suggests new dimensions of solidification process for *nano* solid drug dispersions and it would be very surprising for the pharma world. The solid-liquid interface energy (σ), grain boundary energy (σ_{gb}) and the Gibbs-Thomson coefficient (τ)of all drug alloys have also been discussed. Interface morphology of the alloys follows the Jackson's surface roughness (α) theory and predicts the faceted growth ($\alpha > 2$) proceeds in all the cases.

Keywords: phase diagram, thermodynamic excess and mixing functions, critical radius, interfacial energy, roughness parameter

Introduction

Nicotinamide is a water soluble vitamin B_3, a component of the vitamin B complex group. It was first time clinically used in measuring pellagra preventive factors, PPF (Tanner, 1951) and in treatment of patients undergoing radiation therapy (Jordahl et al., 1961) for lung tumors caused by Mycobacterium Tuberculosis. Intake of nicotinamide for the treatment of HIV-positive patients was suggested 3g per day as tolerable dose (Murray et al., 2001). In addition it has not been shown to produce the flushing, itching and burning sensations of the skin as is commonly seen when large doses of niacin are

administrated orally. Nicam gel (Hakozaki et al., 2002) is most effective when applied to the skin, which helps to reduce the inflammation and redness of inflammatory acne. With material chemistry point of view, it has been a great dream of scientists for a long time to find the techniques which control the properties of solidified structures because the structure formed immediately after solidification determines the properties of the final products. As a number of difficulties encountered working with metallic systems, the transparent model (Bayram et al., 2012; Gupta et al., 2012) is being investigated for observing solidification phenomena with great enthusiasm all over the world. It has been found that at small driving forces, the existence of growth interface leads the stepwise while sufficiently high driving forces is responsible to advance the surface uniformly. With view to achieve better drug products in binary form, the transparent and pharmaceutical active compound nicotinamide (NA) has been taken with Thiourea (TU) as binary system for detailed thermal and solidification behavior such as phase diagram, excess and mixing thermodynamic function, activity and activity coefficient, interfacial energy (σ), surface roughness (α), driving force of solidification (ΔG_v) and critical radius.

Experimental details

Nicotinamide (Thomas Baker, Bombey) and Thiourea (Loba, India) were directly taken for investigation. The melting point (experimental value) of nicotinamide was found 128°C while for Thiourea was found 182°C, respectively. The solid-liquid equilibrium data of NA-TU system were determined by the thaw-melt method (Shekhar et al., 2010; Rastogi & Rama Verma, 1956). Mixtures of different composition were made in glass test tubes by repeated heating and followed by chilling in ice. The melting and thaw temperatures were determined in a Toshniwal melting point apparatus using a precision thermometer which could read correctly up to ± 0.1°C. The heater was regulated to give above 1°C increase in temperature in every five minutes. Heat of fusion of materials was measured by the DTA method using NETZSCH Simultaneous Thermal Analyzer, STA 409 series unit. All the runs were carried out with heating rate 2°C/min, chart speed 10mm/min and chart sensitivity 100μv/10mv.The sample weight was 5 mg for all estimation. Using benzoic acid was a standard substance, the heat of fusion of unknown compound was determined (Krajewska-Cizio, 1990; Shekhar& Kant, 2013a) using the following equation:

$$\Delta H_x = \frac{\Delta H_s W_s A_x}{W_s A_x}$$

where ΔH_x is the heat of fusion of unknown sample and ΔH_s is the heat of fusion of standard substance. W and A are weight and peak area, respectively and suffices x and s indicate the corresponding quantities for the unknown and standard substances, respectively.

Results and discussion

Thermodynamic study

Phase diagram

Solid-liquid equilibrium data of NA-TU system determined by the thaw melt method, is reported (Table 1) in the form of temperature-composition curve in Fig.1. The system shows the formation of 1:5 additive co-crystal at 161°C and two side by side eutectic solid dispersions E2(mole fraction 0.407 of TU) and E1(mole fraction0.968 of TU) at 142°C and 116°C respectively. The congruent melting and a sharp inclination in the intermediate region or at the top of the curve in the diagram suggest the stability and actual stoichiometry of the compound formed. The presence of the addition compound actually produces a phase diagram which consists two separate systems there are three different solid phases namely NA, TU and A1:5 (NA:TU). There will be three fusion curves, $T_{NA}E_2$, $T_{TU}E_1$ and $E_2A1{:}5E_1$ along which solids NA, TU and A1:5 are in equilibrium with the liquid phases at different temperatures. At this temperature the two components has become one component because both solid and liquid phases contain only one compound.

Table 1. Phase composition, melting temperature, values of enthalpy of fusion(ΔH), entropy of fusion (ΔS) and roughness parameter(A)

Alloy	χ_{TU}	MP (°C)	ΔH (J/mol)	DS (J/ mol/K)	α	σ × 10^2 (J/m^2)	s_{gb}× 10^2 (J/m^2)	DS_v (kJ/ m^3/K)	τ × 10^5 Km
E1	0.968	142	17888.32	43.104	5.185	4.819	9.310	780	1.193
A1	0.949	144	18035.76	43.251	5.202	4.823	9.317	774	1.203
A2	0.935	153	18144.40	42.592	5.123	4.825	9.321	756	1.233
A(1:5)	0.835	161	18920.40	43.595	5.244	4.844	9.357	731	1.280
A3	0.789	158	19277.36	44.727	5.380	4.853	9.375	731	1.282
A4	0.706	153	19921.44	46.764	5.625	4.871	9.409	732	1.286
A5	0.616	138	20619.84	50.170	6.034	4.891	9.448	750	1.259
A6	0.517	124	21388.08	53.874	6.480	4.914	9.493	768	1.236
E2	0.407	116	22241.68	57.177	6.877	4.941	9.545	775	1.232
A7	0.384	117	22420.16	57.488	6.915	4.946	9.556	771	1.239
A8	0.286	120	23180.64	58.984	7.095	4.971	9.603	758	1.266
A9	0.151	123	24228.24	61.182	7.359	5.006	9.671	744	1.300
NA		128	25400.00	63.342	7.619	5.046	9.748	726	1.343
TU		182	17640.00	38.769	4.663	4.814	9.300	716	1.300

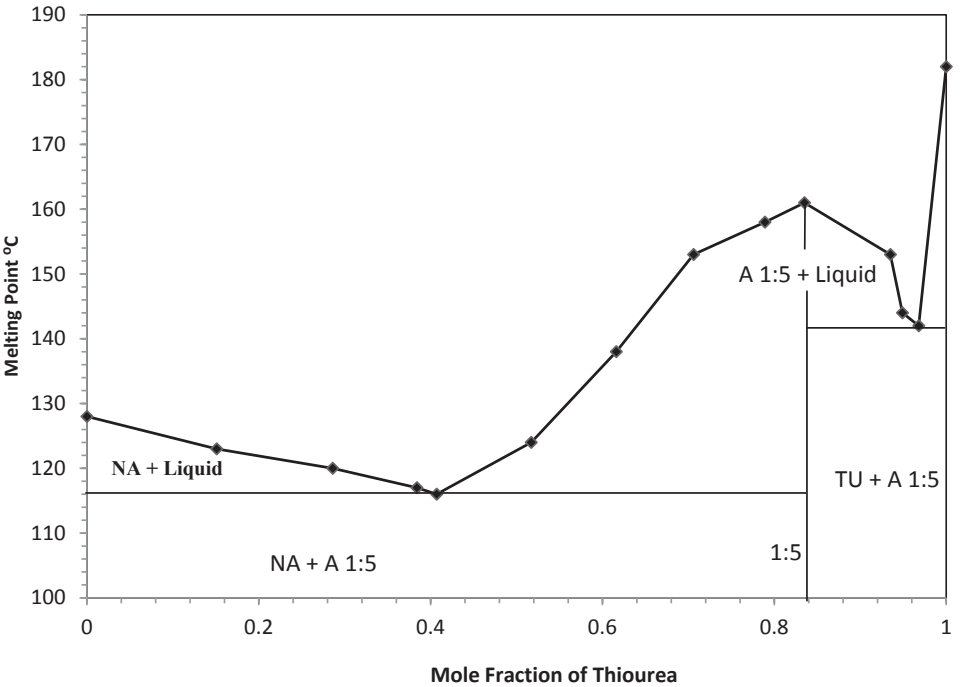

Fig 1. Phase diagram of Nicotinamide(NA)-Thiourea(TU)

Heat of fusion

The values of heats of fusion of eutectic and non-eutectic solid dispersions are calculated by the mixture law using Eq. (1):

$$(\Delta H)_e = \chi_{NA}\ \Delta H_{NA} + \chi_{TU}\ \Delta H_{TU} \qquad (1)$$

where χ and ΔH are the mole fraction and the heat of fusion of the component indicated by the subscript, respectively. The values of heat of fusion of binary products A1-A9, E1 and E2 are reported in Table 1.

Mixing functions

Integral molar free energy of mixing (ΔG^{M}), molar entropy of mixing (ΔS^{M}) and molar enthalpy of mixing (ΔH^{M}) and partial thermodynamic mixing functions of the binary alloys when two components are mixed together were determined by using the following equations:

$$\Delta G^{M} = RT\,(\chi_{NA}\ln a^{l}_{NA} + \chi_{TU}\ln a^{l}_{TU}) \qquad (2)$$

$$\Delta S^{M} = -R\,(\chi_{NA} \ln x^{l}_{NA} + \chi_{TU} \ln \chi^{l}_{TU}) \quad (3)$$

$$\Delta H^{M} = RT\,(\chi_{NA} \ln \gamma^{l}_{NA} + \chi_{TU} \ln \gamma^{l}_{TU}) \quad (4)$$

$$G^{-}_{i}{}^{M} = \mu^{-}_{i}{}^{M} = RT \ln a^{l}_{i} \quad (5)$$

where $G^{-}_{i}{}^{M}$ ($\mu^{-}_{i}{}^{M}$)is the partial molar free energy of mixing of component i (mixing chemical potential) in binary mixture and $\gamma_i$and a_i is the activity coefficient and activity of component respectively. The negative value (Shekhar & Salim, 2011; Nieto et al., 1999) of integral molar free energy of mixing of all the eutectic and non-eutectic alloys (Table 2) suggests that the mixing in all cases is spontaneous. The integral molar enthalpy of mixing value corresponds to the value of excess integral molar free energy of the system favors the regularity in the binary solutions.

The activity coefficient/activity of components for the systems has been calculated from Eq. (6) (Sangster, 1994):

$$- ln\chi_i^l \gamma_i^l = \frac{\Delta H_i}{R}\left(\frac{1}{T_e} - \frac{1}{T_i}\right) \quad (6)$$

where γ^{l}_{i} is activity coefficient of the component *i* in the liquid phase respectively, ΔH_i is the heat of fusion of component i at melting point T_i and R is the gas constant. T_e is the melting temperature of alloy. Using the values of activity and activity coefficient of the components in alloys mixing and excess thermodynamics functions have been computed.

Table 2 Value of partial and integral mixing of Gibbs free energy (ΔG^{M}), enthalpy (ΔH^{M}) and entropy(Δs^{M}) of NA-TU system

Alloy	$\Delta G_{NA}{}^{-M}$ J/mol	$\Delta G_{TU}{}^{-M}$ J/mol	ΔG^{M} J/mol	$\Delta H_{NA}{}^{-M}$ J/mol	$\Delta H_{TU}{}^{-M}$ J/mol	ΔH^{M} J/mol	$\Delta S_{NA}{}^{-M}$ J/mol/K	$\Delta S_{TU}{}^{-M}$ J/mol/K	ΔS^{M} J/mol/K
E1	886.78	-1550.77	-1472.77	12762.82	-1438.55	984.11	28.62	0.27	1.18
A1	1013.47	-1473.23	-1346.41	11330.83	-1291.75	648.00	24.74	0.44	1.68
A2	1583.54	-1124.31	-948.30	11264.49	-886.27	96.47	22.73	0.56	2.00
A3	1900.25	-930.46	-333.18	7475.55	-81.25	-1513.20	12.94	1.97	4.28
A4	1583.54	-1124.31	-328.20	5919.28	108.72	-1817.00	10.18	2.89	5.04
A5	633.42	-1705.85	-807.57	3903.92	-50.26	-1468.10	7.96	4.03	5.54
A6	-253.37	-2248.62	-1284.91	2148.65	-71.13	-1001.00	6.05	5.49	5.76
E2	-760.10	-2558.77	-1492.16	929.94	348.54	-693.31	4.34	7.47	5.62
A7	-696.76	-2520.00	-1396.88	874.24	583.40	-762.56	4.03	7.96	5.54
A8	-506.73	-2403.69	-1049.26	593.96	1686.32	-906.38	2.80	10.41	4.98
A9	-316.71	-2287.38	-614.28	222.24	3936.71	-783.12	1.36	15.72	3.53

Excess thermodynamic functions

With a view to have a quantitative idea and nature of molecular interactions between the components forming the eutectic and non-eutectic alloys and addition compound, the excess thermodynamic functions such as excess integral free energy (g^E), integral excess entropy (s^E) and integral excess enthalpy (h^E) were calculated using Eqs. (7) - (10):

$$g^E = RT(\chi_{NA} \ln \gamma^l_{NA} + \chi_{TU} \ln \gamma^1_{TU}) \tag{7}$$

$$s^E = -R\left((\chi_{NA} \ln \gamma^1_{NA} + \chi_{TU} \ln \gamma^1_{TU} + \chi_{NA} T \frac{\delta \ln \gamma^1_{NA}}{\delta T} + \chi_{TU} T \frac{\delta \ln \gamma^1_{TU}}{\delta T} \right) \tag{8}$$

$$h^E = -RT^2 \left(\chi_{NA} \frac{\delta \ln \gamma^1_{NA}}{\delta T} + \chi_{TU} \frac{\delta \ln \gamma^1_{TU}}{\delta T} \right) \tag{9}$$

and excess chemical potential or excess partial Gibbs free energy

$$g_i^{-E} = \mu_i^{-E} = RT \ln \gamma^1_i \tag{10}$$

Table 3. Value of partial and integral excess Gibbs free energy (g^E), enthalpy (h^E) and entropy (s^E) of NA-TU system

Alloy	g_{NA}^{-E} J/mol	g_{TU}^{-E} J/mol	g^E J/mol	h_{NA}^{-E} J/mol	h_{TU}^{-E} J/mol	h^E J/mol	s_{NA}^{-E} J/mol/K	s_{TU}^{-E} J/mol/K	s^E J/mol/K
E1	12762.82	-1438.55	-984.11	422062.08	-2847.87	10749.25	986.26	-3.40	28.27
A1	11330.83	-1291.75	-648.00	116336.58	-10023.00	-3578.63	251.81	-20.94	-7.03
A2	11264.49	-886.27	-96.47	90660.88	-9571.60	-3056.49	186.38	-20.39	-6.95
A3	7475.55	-81.25	1513.23	84392.67	11721.54	27055.15	178.46	27.39	59.26
A4	5919.28	108.72	1817.03	25919.44	3730.98	10254.39	46.95	8.50	19.81
A5	3903.92	-50.26	1468.15	-895.99	-2364.77	-1800.76	-11.68	-5.63	-7.95
A6	2148.65	-71.13	1001.02	1729.63	7705.48	4819.15	-1.06	19.59	9.62
E2	929.94	348.54	693.31	6423.34	28726.69	15500.80	14.12	72.95	38.07
A7	874.24	583.40	762.56	-4871.44	15291.23	2871.03	-14.73	37.71	5.41
A8	593.96	1686.32	906.38	46537.76	161952.90	79546.48	116.91	407.80	200.10
A9	222.24	3936.71	783.12	28347.81	284557.90	67035.54	71.02	708.64	167.30

The values of $d\ln g_i^l / dT$ can be determined by the slope of liquids curve near the alloys form in the phase diagram. The values of the excess thermodynamic functions are given in Table 3. The value of the excess free energy is a measure of the departure of the system from ideal behavior. The reported excess thermodynamic data substantiate the earlier conclusion of an appreciable interaction during the formation of alloys. The negative value of excess free energy for A1, A2 and E1 indicates the possibility of a stronger association between unlike molecules while the positive value for A4-A9 and E2 in the present system suggests an association of weaker nature between unlike molecules and of stronger nature between like molecules. The maximum negative g^E value for eutectic (Wisniak & Tamir,

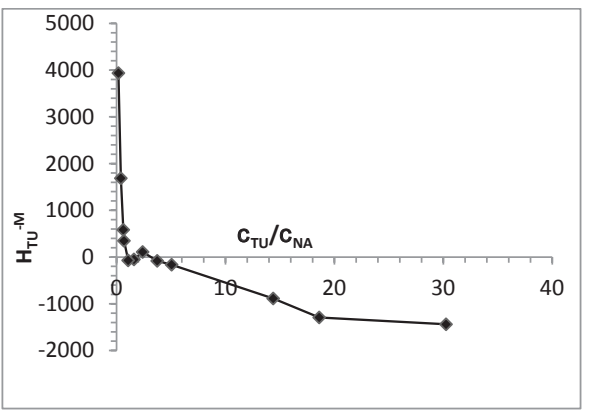

Fig. 2. Graphical solution of partial molar enthalpy of mixing of TU in binary mixture

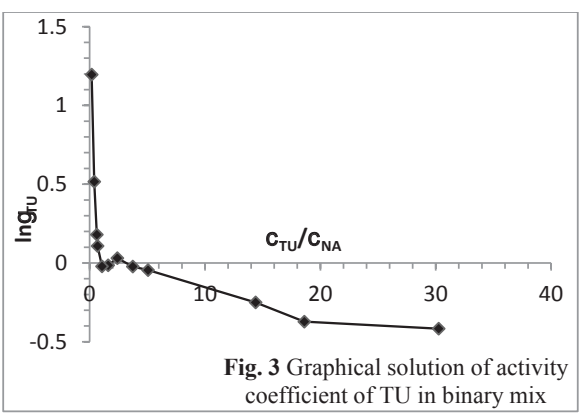

Fig. 3. Graphical solution of activity coefficient of TU in binary mixture

1978; Sharma et al., 2009) alloy E1 infers stronger interaction between NA and TU in the eutectic. The excess entropy is a measure of the change in configurational energy due to a change in potential energy and indicates an increase in randomness.

Gibbs-Duhem equation

The partial molar heat of mixing, activity and activity coefficient can also be determined by using Gibbs-Duhem equation (Shamsuddin et al., 1998):

$$\Sigma \chi_i dz_i^{-M} = 0 \tag{11}$$

or

$$\chi_{NA} dH_{NA}^{-M} + \chi_{TU} dH_{TU}^{-M} = 0 \tag{12}$$

$$dH_{NA}^{-M} = \frac{\chi_{TU}}{\chi_{TU}} dH_{TU}^{-M} \tag{13}$$

$$[\mathrm{H}_{\mathrm{NA}}^{\mathrm{-M}}]_{\chi_{\mathrm{NA}}=y} = \int_{\chi_{NA}=y}^{\chi_{NA}=1} \frac{\chi_{TU}}{\chi_{NA}} dH_{TU}^{-M} \tag{14}$$

Using Eq. (14), a graph (Fig. 2) between H_{TU}^{-M} and χ_{TU}/χ_{NA} gives the solution of the partial molar heat of mixing of a constituent NA in NA/TU alloy and plot between χ_{TU}/χ_{NA} vs $\ln\gamma_{TU}$ determines the value of activity coefficient (Fig. 3) of component NA in binary alloys.

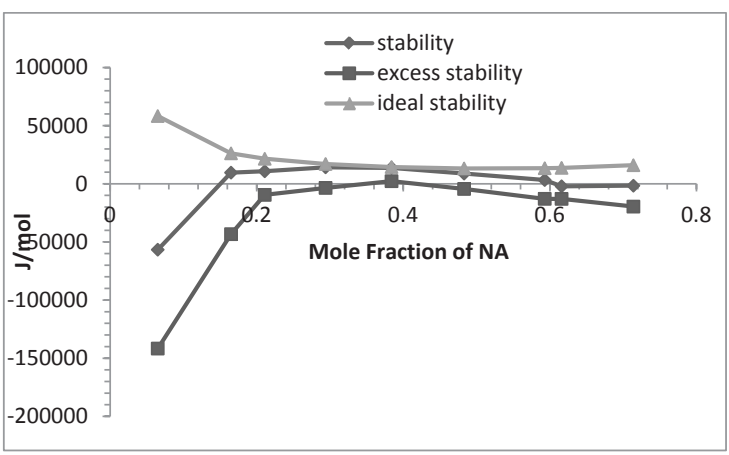

Fig. 4. Stability graph of NA-TU

Stability function

Thermodynamic strength of the present system in form of stability and excess stability functions (Darken, 1967; Shekhar & Kant, 2013) can be determined by the second derivative of their molar free energy and excess energy respectively, with respect to the mole fraction of either constituent:

$$Stability = \frac{\partial^2 \Delta G^M}{\partial \chi^2} = -2RT \frac{\partial \ln a}{\partial (1-\chi)^2} \tag{15}$$

$$Excess\ \ Stability = \frac{\partial^2 g^E}{\partial \chi^2} = -2RT \frac{\partial \ln \gamma}{\partial (1-\chi)^2} \tag{16}$$

These values may be calculated by multiplying the slope (Fig. 4) of ln*a* vs $(1 - x)^2$ and lnγ vs $(1 - x)^2$ plots with -2RT. The best polynomial equation of the curve generated is given below:

$$\gamma=3.68(1-\chi)^2-21.44(1-\chi)^4+81.99(1-\chi)^6-146.84(1-\chi)^8+126(1-\chi)^{10}-41.47(1-\chi)^{12} \tag{17}$$

The slope of the curve shown in Fig. 4 as obtained by differentiating the above equation with respect to $(1 - x)^2$ may also be used to calculate the excess stability of the NA-TU system. The values of total stability to the ideal stability and defined as

$$Ideal\ Stability = \frac{RT}{\chi(1-\chi)} \tag{18}$$

These values show the overall thermodynamic stability in the alloy.

<u>*Interfacial studies*</u>

The effective entropy change (ΔS_v)

The effective entropy change and the volume fraction of phases in the alloy have key role in controlling and deciding the interface morphology during solidification and the volume fraction of the two phases depends on the ratio of effective entropy change of the phases. The entropy of fusion ($\Delta S = \Delta H/T$) value (Table 1) of alloys is calculated by heat of fusion values of the materials. The effective entropy change per unit volume (ΔS_V) is given by

$$\Delta S_V = \frac{\Delta H}{T} \cdot \frac{1}{V_m} \tag{19}$$

where ΔH is the enthalpy change, T is the melting temperature and V_m is the molar volume of solid phase. The entropy of fusion per unit volume (ΔS_V) for NA and TU was found 726 and 716kJK^{-1}m^{-3} respectively. Values of ΔS_V for alloys are reported in Table 1.

The solid-liquid interfacial energy (σ)

An important thermo-physical property is responsible for growth interface. It has been very difficult to measure it with accuracy through experiments and an experimentally observed value of interfacial energy 'σ' keeps a variation of 50-100% from one worker to other. However, Singh & Glickman (1989) had calculated the solid-liquid interfacial energy (σ) from the value of melting enthalpy change and values obtained were found in good agreement with the experimental values. Turnbull empirical relationship (Turnbull, 1950) between the interfacial energy and enthalpy change provides the clue to determine the interfacial energy value of alloy and is expressed as:

$$\sigma = \frac{C\Delta H}{(N)^{1/3}(V_m)^{2/3}} \tag{20}$$

where the coefficient C lies between 0.33 to 0.35 for nonmetallic system, V_m is molar volume and N is the Avogadro's constant. The value of the solid-liquid interfacial energy of nicotinamide and thiourea was found to be 5.046 x $10^{-02}$and 4.814 x 10^{-02} Jm^{-2} respectively and σ value of alloys was given in Table 1.

Interfacial energy can also be calculated by using Gibbs-Thomson coefficient (τ). For a planar grain boundary on planar solid-liquid interface the τ value coefficient for the system can be calculated by the Gibbs-Thomson equation is expressed as

$$\tau = r\Delta T = \frac{TV_m\sigma}{\Delta H} = \frac{\sigma}{\Delta S_V} \tag{21}$$

where τ is the Gibbs-Thomson coefficient, ΔT is the dispersion in equilibrium temperature and, r is the radius of grooves of interface. The theoretical basis of determination of τ was made for equal thermal conductivities of solid and liquid phases for some transparent materials. It was also determined by the help of Gunduz & Hunt (1989) numerical method for materials having known grain boundary shape, temperature gradient in solid and the ratio of thermal conductivity of the equilibrated liquid phases to solid phase ($R = K_L/K_S$).The Gibbs-Thomson coefficient for NA, TU and their alloys are found in the range of 1.193-1.343x10^{-05} *K*m and is reported in Table 1.

The driving force of nucleation (ΔG_v)

The various solidification processes have been focused in the light of diffusion model, kinetic theory of nucleation and thermodynamic laws. Previously it has been explained that the lateral motion of rudimentary steps in liquid advances stepwise/ non-uniform surface at low driving force while continuous and uniform surface advances at suffi-

Table 4. Value of volume free energy change (ΔG_v) during solidification for NA - TU system at different undercoolings (ΔT)

Alloy ↓ / ΔT →	ΔG_v (kJ/m^3)					
	1.0	**1.5**	**2.0**	**2.5**	**3.0**	**3.5**
E1	0.780	1.171	1.561	1.951	2.341	2.731
A1	0.774	1.161	1.548	1.936	2.323	2.710
A2	0.756	1.134	1.512	1.890	2.269	2.647
A(1:5)	0.731	1.097	1.462	1.828	2.193	2.559
A3	0.731	1.097	1.463	1.828	2.194	2.560
A4	0.732	1.098	1.464	1.830	2.196	2.562
A5	0.750	1.125	1.500	1.876	2.251	2.626
A6	0.768	1.152	1.536	1.920	2.304	2.688
E2	0.775	1.162	1.550	1.937	2.325	2.712
A7	0.771	1.157	1.542	1.928	2.314	2.699
A8	0.758	1.137	1.517	1.896	2.275	2.654
A9	0.744	1.116	1.488	1.860	2.232	2.604
NA	0.726	1.089	1.452	1.815	2.178	2.541
TU	0.716	1.073	1.431	1.789	2.147	2.505

Table 5. Critical size of nucleus (r^*) at different undercoolings (ΔT)

Alloy ↓ / ΔT →	r*(nm)					
	1.0	**1.5**	**2.0**	**2.5**	**3.0**	**3.5**
E1	123.5	82.34	61.76	49.41	41.17	35.29
A1	124.6	83.05	62.29	49.83	41.53	35.60
A2	127.6	85.08	63.81	51.05	42.54	36.46
A(1:5)	132.5	88.34	66.26	53.01	44.17	37.86
A3	132.7	88.47	66.35	53.08	44.24	37.92
A4	133.1	88.73	66.55	53.24	44.37	38.03
A5	130.4	86.92	65.19	52.15	43.46	37.25
A6	128.0	85.30	63.98	51.18	42.65	36.56
E2	127.5	85.01	63.75	51.00	42.50	36.43
A7	128.3	85.52	64.14	51.31	42.76	36.65
A8	131.1	87.40	65.55	52.44	43.70	37.46
A9	134.6	89.72	67.29	53.83	44.86	38.45
NA	139.0	92.66	69.49	55.60	46.33	39.71
TU	134.6	89.70	67.28	53.82	44.85	38.44

ciently high driving force. The driving force of nucleation during solidification (ΔG_V) is determined at under cooling (ΔT) by using of Eq. (22) (Hunt & Lu, 1994):

$$\Delta G_V = \Delta S_v \Delta T \tag{22}$$

It is opposed by the increase in surface free energy due to creation of a new solid-liquid interface. By assuming that solid phase nucleates as small spherical cluster of radius arising due to random motion of atoms within liquid. The value of ΔG_V is shown in the Table 4.

The critical size of nucleus (r)*

It is well known that during liquid-solid transformation embryos (unstable nucleus) are rapidly dispersed in unsaturated liquid and on undercooling liquid becomes saturated and provides particles with stable nucleus corresponding to size of critical nucleus which is responsible for the nucleation and growth of crystal. The radius of critical nucleus / critical size of nucleus (r*) can be expressed by the Chadwick (1972) relation

Table 6. Value of critical free energy of nucleation (ΔG^*) for alloys of NA-TU system at different undercooling (ΔT)

Alloy ↓ → **ΔT**	**ΔG*×10^{16} (J/molecule)**					
	1.0	**1.5**	**2.0**	**2.5**	**3.0**	**3.5**
E1	30.81	13.69	7.70	4.93	3.42	2.52
A1	31.37	13.94	7.84	5.02	3.49	2.56
A2	32.93	14.64	8.23	5.27	3.66	2.69
A(1:5)	35.64	15.84	8.91	5.70	3.96	2.91
A3	35.81	15.92	8.95	5.73	3.98	2.92
A4	36.16	16.07	9.04	5.79	4.02	2.95
A5	34.84	15.48	8.71	5.57	3.87	2.84
A6	33.71	14.98	8.43	5.39	3.75	2.75
E2	33.66	14.96	8.42	5.39	3.74	2.75
A7	34.11	15.16	8.53	5.46	3.79	2.78
A8	35.81	15.91	8.95	5.73	3.98	2.92
A9	38.00	16.89	9.50	6.08	4.22	3.10
NA	40.85	18.15	10.21	6.54	4.54	3.34
TU	36.52	16.23	9.13	5.84	4.06	2.98

$$r^* = \frac{2\sigma}{\Delta G_V} = \frac{2\sigma T}{\Delta H_V \Delta T} \tag{23}$$

where σ is the interfacial energy and ΔH_V is the enthalpy of fusion of the compound per unit volume, respectively. The critical size of the nucleus for the components and alloys was calculated at different undercoolings and values are presented in Table 5. It can be inferred from table that the size of the critical nucleus decreases with increase in the undercooling of the melt. The existence of embryo and a range of embryo size can be expected in the liquid at any temperature.

Further it has been observed that during critical nucleus formation, a localized critical free energy of nucleation (ΔG*) is required which is evaluated (Wilcox, 1974) as

$$\Delta G^* = \frac{16}{3} \frac{\pi \sigma^3}{\Delta G_v^2} \tag{24}$$

The value of ΔG^* has been found in the range of 10^{-15} to 10^{-16} J per molecule at undercoolings 1-3.5°K, and has been reported in Table 6.

Interfacial Grain boundary energy (σ_{gb})

During in liquid-solid transformation nucleation and growth on internal surfaces gives the idea about fundamentals of grain boundary. In past, a numerical method (Akbulut et al., 2009) is applied to observe the interfacial grain boundary energy (σ_{gb}) without applying the temperature gradient for the grain boundary groove shape. For isotropic interface there is no difference in the value of interfacial tension and interfacial energy. A considerable force is employed at the grain boundary groove in anisotropic interface. The grain boundary energy can be obtained by the equation:

$$\sigma_{gb} = 2\sigma \cos\theta \tag{25}$$

where θ is equilibrium contact angle precipitates at solid-liquid interface of grain boundary. The grain boundary energy could be twice the solid-liquid interfacial energy in the case where the contact angle tends to zero. The value of σ_{gb} for solid NA and TU was found to be 9.748 x $10^{-2}$and 9.300 x 10^{-2}Jm^{-2} respectively and the value for all alloys is given in Table 1.

Interface morphology

The solid-liquid interface morphology can be predicted from the value of the entropy of fusion. According to Hunt & Jackson (1966), the type of growth from a binary melt

depends upon a factor α which is almost the entropy of fusion in dimensionless unit, defined precisely:

$$\alpha = \xi \frac{\Delta H}{RT} = \xi \frac{\Delta S}{R} \tag{26}$$

where ξ $\{T_c/T = (T - \Delta T)/T\}$ is a crystallographic factor depending upon the geometry of the molecules and has a value less than or equal to one. $\Delta S/R$ (also known as Jackson's roughness parameter α) is the entropy of fusion (dimensionless) and R is the gas constant. When α is less than 2 for both phases the solid-liquid interface essentially grow from the melt isotropically with no crystalline facets transforming the melt into regular crystalline morphology and becomes atomically rough and exhibits non-faceted growth. Irregular interface appears when $\alpha > 2$ for both phases, which concurrently initiate the anisotropic growth with crystalline facets. The non-faceted crystal holds a round growth front while the faceted crystal poses a sharp growth front. The computed α values for nicotinamide and Thiourea respectively are on the order of 7.619 and 4.663revealing the faceted morphology of the binary composite material. The liquid-solid growth habits of the overall binary products due to their high entropies of fusion are greatly influenced by thermal and mechanical stresses and split into groups of crystals that give rise to a regular morphology. The value of Jackson's roughness parameter ($\Delta S/R$) is given in Table 1. For all the alloy the α value was found greater than 2 which indicates the faceted (Shekhar, & Salim, 2011) growth proceeds in all the cases.

Acknowledgement: Thanks are due to the Head Department of Chemistry, V K S University, Ara 802301, India, for providing research facilities.

REFERENCES

Akbulut, S., Ocak, Y., Keşlioğlu, K. &Maraşli, N. (2009).Determination of interfacial energies in the aminomethylpropanediol-neopentylglycol organic alloy. *Appl. Surf. Sci., 255,* 3594-3599.

Bayram, **Ü.,** Aksöz, S. & Maraşlı, N. (2012). Dependency of thermal conductivity on the temperature and composition of D-camphor in the neopentylglycol–D-camphor alloys. *Thermochemica Acta. 531*, 12-20.

Chadwick, G.A. (1972). *Metallography of phase transformation*. London: Butterworths.

Darken, L.S. (1967). Thermodynamics binary metallic solutions. *Trans. Met. Soc. AIME. 239,* 80-89.

G**ü**nd**ü**z, M. & Hunt, J.D. (1989).Solid-liquid surface energy in the Al-Mg system. *Acta Metallurgica, 37,* 1839-1845.

Gupta, P., Agrawal, T., Das, S.S. & Singh, N.B. (2012). Phase equilibria and molecular interaction studies on (naphthols + **vanillin) systems**. *J. Chem. Therm.48*, 291-299.

Hakozaki, T., Minwalla, L.Chhoa, M., Matsubara, A., Miyamoto, K., Greatens, A., Hillebrand, C.G., Bissett, D.L. & Boissy, R.E. (2002). The effect of niacinamide on reducing cutaneous pigmentation and suppression of melanosome transfer. *British J. Dermatol*., *147*, 20-31.

Hunt, J.D. & Jackson, K.A. (1966). Binary eutectic solidification. *Trans. Metall. Soc. AIME, 236,* 843-852.

Hunt, J.D. & Lu, S.-Z. (1994). Crystallization of eutetics, monotetics and peritetics (pp. 1111-1166). In: Hurle, D.T.J. (Ed.). *Handbook on crystal growth 2: bulk crystal growth. Part B: Growth mechanisms and dynamics.* Amsterdam: North-Holland.

Jordahl, C., DesPrez, R., Deuschle, K. Muschenhelm, C. & McDermott, W. (1961). Ineffectiveness of nicotinamide and isoniazid in treatment of pulmonary tuberculosis. *Am. Rev. Respir. Dis. 83*, 899–900.

Krajewska-Cizio, A. (1990). Phase diagrams in the binary systems of N-isopropylcarbazole with 2,4,7-trinitrofluorene-9-one and carbazole. *Thermochimica Acta, 158*, 317-325.

Murray, M.F., Langan, M. & Mac Gregor, R.R. (2001). Increased plasma tryptophan in HIV-infected patients treated with pharmacologic doses of nicotinamide. *Nutrition, 17,* 654–656.

Nieto, R., González, M.C. & Herrero, F. (1999).Thermodynamics of mixtures: function of mixing and excess functions. *Amer. J. Phys., 67,* 1096-1099.

Rastogi, R.P. & Rama Verma, K.T. (1956). Solid-liquid equilibria in solutions of non-electrolytes. *J. Chem. Soc.,* 2097-2101.

Sangster, J. (1994). Phase diagram and thermodynamic properties of binary organic systems based on 1,2- 1,3- 1,4-diaminobenzene or benzidine. *J. Phys. Chem. Ref. Data. 23,* 295-338.

Shamsuddin, M., Singh, S.B. &Nasar, A. (1998). Thermodynamic investigations of liquid gallium-cadmium alloys. *Thermochemica Acta. 316*, 11-19.

Sharma, B.L., Tandon, S. & Gupta, S. (2009). Characteristics of the binary faceted eutectic; benzoic acid- salicylic acid system. *Cryst. Res. Technol., 44,* 258-268.

Shekhar, H. & Kant, V. (2013a). Thermal and interfacial studies of binary alloys of nicotinamide - β-naphthol drug system. *Asian J. Chem., 25,* 2441-2446.

Shekhar, H. & Kant, V. (2013b). *Thermodynamics of nicotinamide based binary drug systems.* Saarbrücken: Lambert Academic Publishing.

Shekhar, H. & Salim, S.S. (2011). Molecular interactions and stability in binary organic alloys. *J. Nat. Acad. Sci. Lett., 34,* 117-125.

Shekhar, H., Pandey, K.B. & Kant, V. (2010). Thermodynamic characteristics of 1:2

molecular complex of phthalic anhydride-camphene system. *J. Nat. Acad. Sci. Lett., 33*, 153-160.

Singh, N.B. & Glicksman, M.E. (1989). Determination of the mean solid-liquid interface energy of pivalic acid. *J.Cryst. Growth, 98,* 573-580.

Tanner, E. (1951). Über den Versuch einer neuer medikamentosen Therapie der Bronchustuberkulose. *Helv Med Acta*, *18,* 456-460.

Turnbull, D. (1950). Formation of crystal nuclei in liquid metals. *J. Chem. Phys., 21*, 1022-1028.

Wilcox, W.R. (1974). The relation between classical nucleation theory and the solubility of small particles. *J. Crystal Growth, 26,* 153-154.

Wisniak, J. & Tamir, A. (1978).*Mixing and excess thermodynamic properties: a literature source book*. *Vol. 1*.New York: Elsevier.

✉**Vishnu Kant** and **H. Shekhar**
Department of Chemistry
VKS University
Ara – 802301, India
E-mail: imvishnukant@gmail.com
E-mail: hshe2503@rediffmail.com